

## Some geodynamic aspects of Kutch basin and seismicity: An insight from gravity studies

D. V. Chandrasekhar and D. C. Mishra\*

National Geophysical Research Institute, Hyderabad 500 007, India

The Bouguer anomaly of Kutch shows several gravity highs and lows, primarily attributed to fault-controlled basement uplifts and depressions. Gravity modelling suggests larger thickness of sediments towards the south and a general uplift of basement towards the north, descending stepwise towards the south indicating post-rift vertical tectonics. This might be responsible for the basement uplifts controlled by thrust faults with about 2–3 km upthrow. However, their listric nature dipping towards the south in depth suggests that horizontal forces due to plate movement may have also contributed to their evolution. Circular gravity highs observed over islands (uplifts) in the northern part of Kutch along Island Belt Fault and their modelling suggest high-density rocks at the basement, which may represent volcanic plugs or subsurface mafic rocks. The isostatic regional derived from the Bouguer anomaly map provides two centres of mass deficiencies in this region located under the SE part of the Kutch Mainland Uplift (KMU) and the Wagad uplift separated by a NW–SE trend coinciding with the strike slip fault, west of the Wagad uplift. Crustal thickness model based on isostatic regional varies from 35 km along the coast to 44 km under the SE part of KMU and Wagad uplift, which is controlled by faults and suggests isostatic overcompensation. The Bhuj earthquake of 26 January 2001 and its aftershocks are concentrated in the zone of intersection of the thrust faults: Kutch Mainland fault, south and north Wagad fault and NW–SE and NE–SW structural trends, which are delineated based on gravity anomalies. The isostatic overcompensation causes differential uplift and erosion, resulting in vertical stress. This along with the horizontal stress resulting from the movement of the Indian plate might be responsible for large magnitude and relatively frequent earthquakes in this region.

KUTCH represents the northernmost part of the Atlantic-type, western passive margin of India and lies close to the western convergent boundary of the Indian plate with the Eurasian plate<sup>1</sup>. The NE–SW movement of the Indian plate due to spreading at the Carlsberg ridge provides a horizontal force to the Indian plate, which creates stress in the different sections especially along its contact with the Eurasian plate and nearby. Kutch basin has received much attention in the past for its unbroken, richly fossiliferous Jurassic rocks and has fascinated earth scien-

tists for a long time after the 1819 Kutch earthquake. The Kutch basin on the western continental margin is related to the break-up of Africa from Greater India from erstwhile Gondwanaland during middle Jurassic<sup>2</sup>. The rifting took place in stages by a series of sub-parallel latitudinal faulting along primordial tectonic trends from north to south. The rifting was aborted by early Cretaceous when Kutch basin got filled with clastics of prograding delta as the sea regressed and the rifting subsequently shifted towards Cambay and Narmada grabens in the south (inset, Figure 1). The Kutch basin is typically a continental margin basin embayed into rifted graben. It is an E–W oriented Mesozoic rift basin bounded by Nagar Parker fault in the north and Kathiawar uplift fault towards the south (inset, Figure 1). The Kutch basin presents the sediments from middle Jurassic to Holocene. Much of the sedimentation in the Mesozoic took place during early rift phase of the western continental margin and has thick ( $\geq 3000$  m) Mesozoic sediments followed by relatively thin, about 1000 m, of Tertiary sediments. The Mesozoic (middle Jurassic to early Cretaceous) rocks are exposed extensively on the highland areas (Figure 1), whereas Tertiary sediments are present in the low-lying bordering plain land towards the coast and plains of Rann. Deccan traps of late Cretaceous separate the Mesozoic and Tertiary stratigraphy of Kutch (Figure 1) towards the north and the south respectively. Deccan traps are largely restricted towards the southern part of the Kutch mainland extending from Lakhpat in west to Anjar in the east. Lava flows are generally tholeiitic basalts overlying the Jurassic sandstone occupying the southern and southwestern slopes of the central highland. Some alkaline rocks similar to the volcanic plugs of Deccan trap in Saurashtra have also been reported. The trap gradually thins out northward and is absent in the outcropping areas further north in the island belt (Figure 1), though some exposures of Deccan trap are recently reported from Pachham island by Geological Survey of India. The distribution of traps in Kutch appears to be controlled by the pre-trappean topography, and the central part of the mainland was already elevated and the Mesozoics were already folded, when the trap began to erupt<sup>3</sup>. The important structural features of the Kutch basin are a group of E–W trending uplifts, namely Kutch Mainland Uplift (KMU), Pachham, Khadir, Bela, Wagad and Chorar uplifts (Figure 1) surrounded by residual depressions like Rann of Kutch and Banni plain. All these major uplifts are bounded by a fault or by flexure on one side and gently dipping peripheral plains on the other. The blocks have been tilted, with the northern flanks upthrown. They can be regarded as median uplifts and shoulders of the Kutch rift basin, as generally reported from other rift basins of the world. The KMU is controlled by a major E–W structural fault (F1, Figure 1) known as Kutch Mainland Fault (KMF) in the north, Katrol hill fault (F3) in the south and NW–SE oriented Vigodi fault (F2) in the west (Figure 1).

\*For correspondence. (e-mail: ngrigravity@yahoo.com)

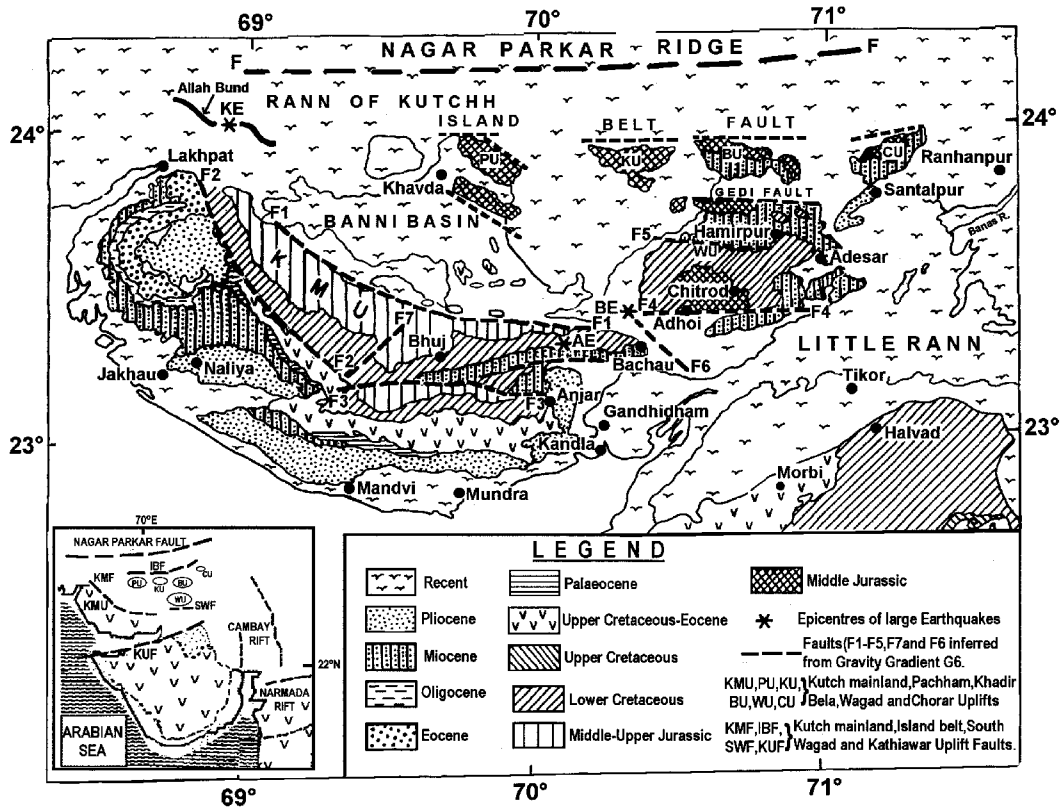


**Figure 1.** Geology and major tectonic of Kutch. F1, F2 and F3 are the northern, western and southern boundary faults of the median uplift. Epicentre of Bhuj earthquake (BE) of 26 January 2001, Anjar earthquake (AE) of 1956 and Kutch earthquake (KE) of 1819 are also plotted. (Inset) Tectonic setting of Kutch rift basin between Nagar Parkar fault and Kathiawar uplift fault and adjoining Cambay and Narmada rift basins. F1, KMF; F2, Vigodi fault; F3, Katrol hill fault and F4, South Wagad fault. F5 is introduced based on gravity gradient G5 (Figure 5). F6, Strike slip fault along the western margin of the Wagad uplift coinciding with a major lineament.

It also shows a Hinze zone in the central part, west of Bhuj<sup>2</sup>. These faults cut through the Mesozoic rocks in this region and play an important role in the geomorphic evolution of the Kutch basin. Similarly, Island Belt fault in the north and sub-parallel faults such as Khavda, Gedi and South Wagad faults (Figure 1) in the south have controlled Pachham, Khadir, Bela, Wagad and Chorar uplifts. The KMF extends about 100 km in NW–SE orientation in the western part of Kutch, changing to the E–W orientation in the central part of Kutch. It is displaced towards north as South Wagad fault F4 (Figure 1). Another fault F5 is the Gedi fault located north of the Wagad uplift. The role of the regional and local tectonics for seismic activity of Kutch has been discussed in detail<sup>4,5</sup>.

Kutch has witnessed several seismic activities in the past; notable among them are the Kutch earthquake of magnitude 8.0 in 1819 (ref. 6) and Anjar earthquake of magnitude 7.0 in 1956 (ref. 7). The epicentre of the Kutch earthquake of 1819 coincides with the Island Belt Fault (IBF, Figure 1), which created an uplift of 5 to 6 m over a length of 80 km known as Allah bund and subsidence<sup>6</sup> south of it. Several historical and pre-historical

earthquakes<sup>8</sup> causing various geomorphological changes such as changes in the river courses, subsidence in Kutch and Saurashtra forming Rann of Kutch, etc. have been reported from this area. At least three seismic activities<sup>9</sup> have been reported from pre-historic Indus Valley Civilization (2900–1800 BC) in Dholavira on Khadir Island (Figure 1). Due to recurrence of large-magnitude earthquakes, this region is placed in zone V on the seismic zoning map of India on par with the Himalaya<sup>10</sup>.

The Bouguer anomaly map of Kutch is prepared based on some earlier data<sup>11</sup> and 275 new gravity observations (Figure 2) in the central and western part of Kutch and Khadir island, where practically no data existed earlier. The survey is carried out using Lacoste–Romberg gravimeter with an accuracy of 0.01 mGal. The new data together with earlier data set are processed using IGSN71 for a Bouguer slab density of 2670 kg/m<sup>3</sup>. The survey is conducted using an electronic altimeter controlled from several benchmarks of Survey of India in this area. As the area is largely flat, it provided an accuracy of 2–3 m in elevation, which causes an inaccuracy of about ±0.5 mGal due to error in elevation. As this is the major source of error in gravity data processing, the computed

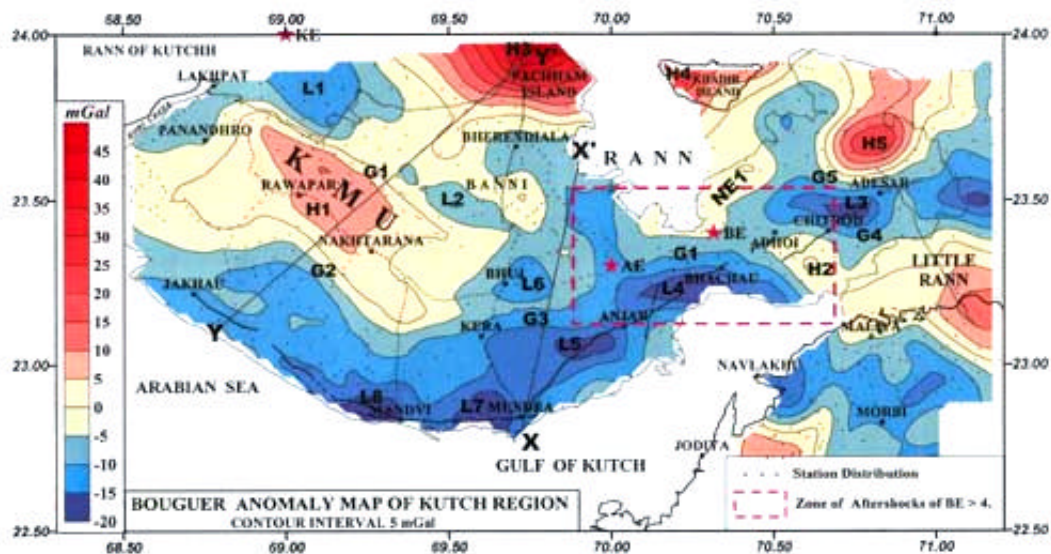


**Figure 2.** Bouguer anomaly map of Kutch. G1–G5 indicate gravity gradients which approximately coincide to faults F1–F5 (Figure 1). H1–H5 and L1–L8 are gravity highs and lows indicating basement uplifts (islands) and depressions. H2 (NW–SE gravity trend) and NE1 are coinciding with the fault F6 (Figure 1) and NE–SW trend delineated based on gravity anomalies. NW–SE and NE–SW gravity trends intersect E–W-oriented gravity trends G1, G4 and G5 representing faults F1, F4 and F5 respectively, in the epicentral area of the Bhuj earthquake (BE) and its aftershocks greater than 4.

Bouguer anomaly will have an accuracy better than  $\pm 1$  mGal. The Bouguer anomaly map (Figure 2) presents a central gravity high H1 with gradients G1, G2 and G3 towards its northern, western and southern margins. As these gradients coincide with the margins of the median uplifts, they appear to represent the reverse faults which have controlled this uplift. These gradients depend on the density contrast across these faults and their extents, which can be judged only through modelling. The eastern margin of the gravity high H1 coincides with the Hinze zone of the KMU between Bhuj and Nakhtarana. There are several gravity highs (H2–H5) and lows (L1–L8), which represent local uplifts and depressions of the basement respectively. The gravity high H2 is a NW–SE oriented trend east of the KMU. The gravity highs H3, H4 and H5 coincide with the Pachham, Khadir and Bela islands, which are almost circular gravity highs of large amplitude of 25–50 mGal. The gravity gradient G1 north of the KMU extends further east (Figure 2) as G4, which represents the southern margin fault of the Wagad uplift. The gravity gradients G1 and G4 are intersected by gravity high H2 striking NW–SE. The gravity gradient G5 separates the Mesozoic sediments of the Wagad uplift from the Tertiary sediments to the north of it (Figure 1). The western margin of the Wagad uplift is bounded by the gravity trend NE1, which is oriented NE–SW and almost coincides with the boundary separating Wagad uplift from the Rann of Kutch. The gravity lows (L1–L8) represent depressions between the uplifts and are primarily caused due to sediments, though they may be part of the uplifts.

The observed Bouguer anomaly is the cumulative effect of attraction due to sources lying at different levels and can be classified into two broad components (i) residual anomalies due to shallower sources, and (ii) regional anomalies due to deeper sources. The topography overlying the sea level is generally compensated at the subsurface level known as the depth of compensation, which generally coincides with the Moho and results in regional anomalies. If the overburden above sea level is fully compensated at the Moho, it is known as isostatically compensated and such regions do not experience any vertical tectonics due to buoyant forces. However, if the areas are overcompensated, implying that the mass deficiency at the Moho is more than the topographic load, the area tends to rise due to buoyant forces till the hydrostatic balance is attained. Therefore, the state of isostasy in a region can effectively be used to understand the nature of vertical forces in any region. The regional component caused by isostatic compensation at the Moho is derived from the observed Bouguer anomaly based on the principles of zero free-air anomaly<sup>12</sup>. Free-air anomaly consists of the effect of both the topographic load and the compensating mass, besides the effect due to shallow sources. Thus, its zero value for regional elevation implies that the two effects have cancelled each other and indicates a fully compensated crust. The effects due to shallow sources are usually represented by short wavelength anomalies and therefore regional elevation is considered, which is a large wavelength feature and involved in compensation. The Bouguer anomaly is computed after correcting for the topography and therefore it con-

sists of only the effect due to compensating mass and shallow sources. Therefore, for a regional elevation, the value of the Bouguer anomaly where free-air anomaly is zero indicates the effect of compensating mass. A profile XX' across the KMU showing Bouguer anomaly, free-air anomaly and elevation is given in Figure 3, to demonstrate the use of zero free-air for evaluating the effect of isostatic compensation. These plots show a positive correlation among elevation, free-air anomaly and Bouguer anomaly, which qualitatively suggests lack of isostatic compensation. The isostatic regional (ZF) is drawn over the Bouguer anomaly (Figure 3a) by joining the Bouguer values for which free-air anomaly is zero (Figure 3b). It shows a gravity low, which suggests a crustal thickening under this section. An isostatic regional map for the whole region prepared based on this principle, i.e. taking the Bouguer anomaly corresponding to free-air anomaly, equal to zero as isostatic anomaly, is shown in Figure 4. It presents two prominent centres of gravity lows A and B of amplitude  $-11$  and  $-13$  concentrating between Bhuj, Mundra and north of Chitrod respectively. They represent the centres of mass deficiency at the Moho, which coincide with the SE part of the KMU and the Wagad uplift. The epicentres of the Bhuj earthquake (BE) and its aftershocks of magnitude greater than four and Anjar earthquake (AE) are located close to these centres of mass deficiencies. The isostatic regional computed here is different from the isostatic gravity anomaly generally computed based on elevation<sup>11</sup>. The former provides the effects of compensating mass, as discussed above, while the latter removes the effect of compensating mass corre-

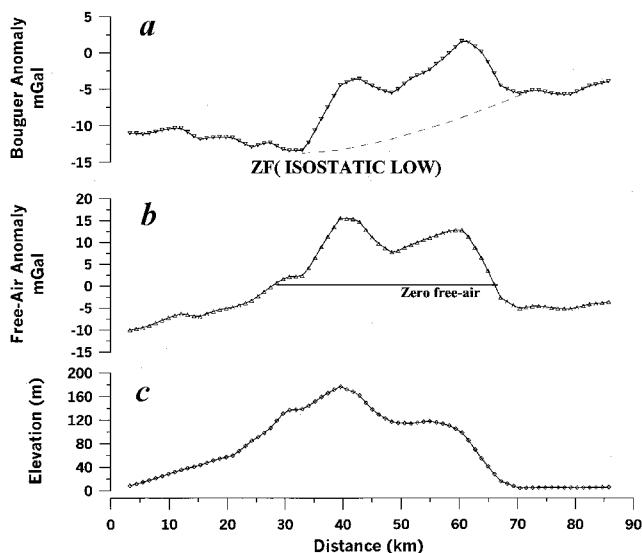


**Figure 3.** Profile XX' (Figure 2) across the KMU showing elevation (c), free-air anomaly (b) and Bouguer anomaly (a). Free-air anomaly and Bouguer anomaly show positive correlation with the regional elevation, indicating lack of isostatic compensation. ZF corresponds to the zero free-air (b) on Bouguer anomaly profile (a), representing the gravity effect due to the compensating mass.

sponding to elevation in the area based on Airy's model; therefore, it provides the effects of shallow sources. The isostatic gravity anomaly<sup>11</sup> therefore, shows in general, regional gravity high in this area corresponding to the KMU and other uplifts of this area.

The residual Bouguer anomaly along the profile XX' (Figure 5) is obtained by subtracting the regional field (Figure 4) from the observed field (Figure 2) along the same profile. This profile is chosen for modelling as it cuts across the gravity gradients G1 and G3, which represent the northern and southern boundary faults of the KMU, and passes through the minimum value of the isostatic regional gravity field (A, Figure 4). The crustal model is prepared (Figure 5) using constraints from the cross-section at Mundra–Bachau for the depth of basement and bulk density of sediments based on integrated geophysical approach<sup>13</sup> and some information from oil wells in the immediate neighbourhood<sup>14</sup>. The residual gravity field is computed for the bulk densities of 2100, 2450 and 2700 kg/m<sup>3</sup> for Tertiary and Mesozoic sediments and the basement respectively<sup>15</sup>. The exposed rock formation with density 2740 kg/m<sup>3</sup> represents Deccan trap, which is the bulk density of this rock reported from laboratory measurements. The densities of Tertiary and Mesozoic sediments are controlled from density logs from the oil wells<sup>14</sup> and laboratory measurements from the surface samples. The basement model shows an uplift of 2 to 3 km across gravity gradients G1 and G3 and represents thrust faults, which correspond to F1 and F3 representing the KMF and the Katrol fault, referred to above (Figure 1). The KMF (F1) is almost vertical, while F3 dips 50–60° with 2–3 km upthrow. The isostatic regional is modelled for a standard crustal thickness of 35 km along the coast and  $-400$  kg/m<sup>3</sup> of density contrast between the lower crust and the upper mantle. The computed model provides 44 km thick crust controlled by sharp contacts on either side, which may represent faults. It may be observed that the gravity lows L5, L6 are basically caused by thickness of sediments compared to adjoining uplifts.

The gravity highs H1 and H3, being the most prominent ones, a gravity profile YY' across these anomalies starting from Jakhau to Pachham island is modelled. The residual Bouguer anomaly (Figure 6) along this profile is obtained by subtracting isostatic regional (Figure 4) from the observed field (Figure 2) along this profile. The residual anomaly is modelled for similar bulk density of Mesozoic sediments (2450 kg/m<sup>3</sup>) and the basement (2700 kg/m<sup>3</sup>), as discussed along profile XX'. The basement model for which the computed field shows a good match with the observed field is shown in Figure 6. The layers with densities 2740 and 2100 kg/m<sup>3</sup> represent exposed Deccan trap and Tertiary sediments respectively. This model also shows that the KMU is controlled by thrust faults towards the north and south, with a maximum throw of 2–3 km on either side. The Vigodi fault F2

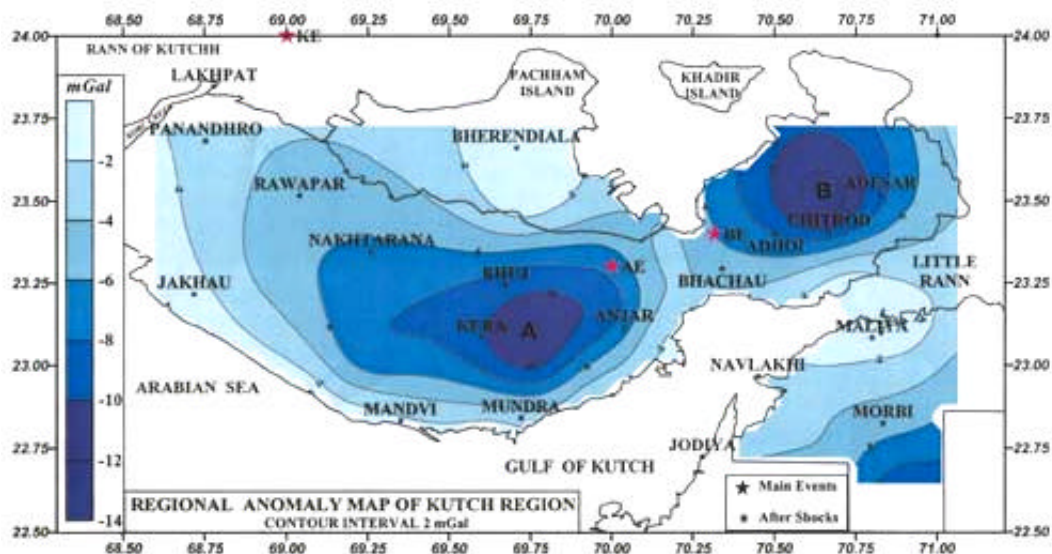


**Figure 4.** Regional isostatic map derived from Figure 2. A and B denote regional gravity lows indicating mass deficiency at the Moho separated by a NW–SE trend between Anjar and Bachau, almost coinciding with the NW–SE trend (H2) in the Bouguer anomaly map (Figure 2). This indicates the deep-seated nature of this trend. The epicentre of the Bhuj and Anjar earthquakes lies between the centres of mass deficiency, causing differential uplift in this region.

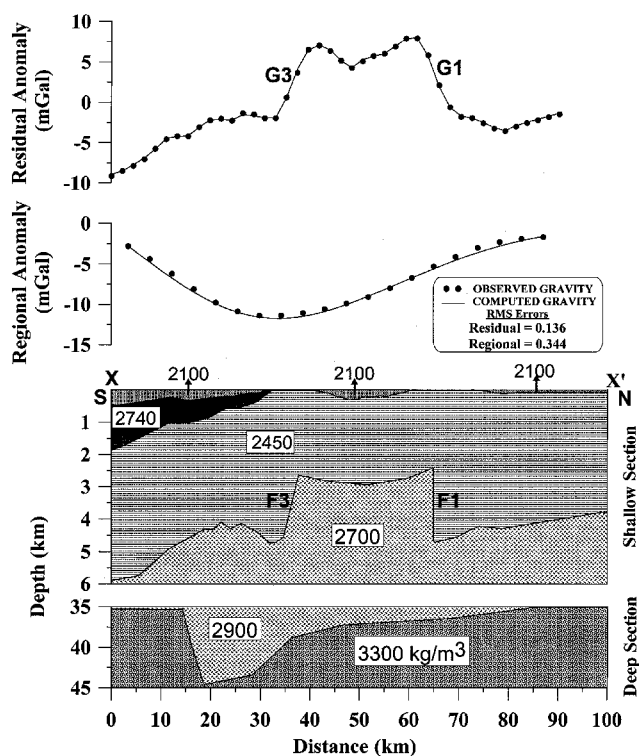


**Figure 5.** Shallow cross-section up to the basement derived from 2D modelling of residual gravity anomaly along a profile XX' (Mundra to Bherendiala) using constraints from seismic and magnetotelluric studies at Mundra<sup>13</sup>. It shows a basement uplift of 2–3 km along F1 and F3. The deeper section is modelled from isostatic regional along the same profile, suggesting a crustal thickening from 35 km along the coast to 44 km under SE part of the KMF controlled by sharp contacts (faults).

towards SW of the KMF appears to be listric in nature, almost vertical at the surface and flattening out in depth. Though the anomaly due to Pachham island is not recorded fully, it shows a basement uplift of 4–5 km under this section. The subsurface high density ( $2800 \text{ kg/m}^3$ ) body under it is required to account for the observed Bouguer anomaly with 0.5–1.0 km of Mesozoic sediments exposed in this area. The Moho configuration along this profile not modelled as the isostatic regional is reduced to a maximum of  $-4.0 \text{ mGal}$  along this profile.

The gravity modelling suggests uplift of basement towards the north along several thrust faults, which are descending towards the south increasing the sedimentary thickness southwards (Figures 5 and 6). Some of these thrust faults are listric in nature (F3, Figure 5) dipping towards the south in depth, which suggests that they must have been influenced due to movement of the Indian plate towards the north. The isostatic regional anomaly map presents two centres of gravity lows over the SE part of KMF and Wagad uplift, indicating mass deficiencies at the Moho level. Their modelling indicates a 8–10 km thick crust beneath, varying from 35 km along the coast to 44–45 km under the KMF controlled by faults. The second centre of gravity low in the isostatic regional anomaly map (Figure 4) being almost of same order, will cause the same order of crustal thickening (44–45 km). The KMF may be connected to the northern fault controlling the Moho under it as a listric fault (Figure 5). Moreover, presence of listric faults in the ductile part of the crust (lower crust) is more common than straight faults.

As the regional elevation is only 150 m, it will produce approximately 1 km of crustal root. Therefore, 8–10 km of crustal thickening suggests overcompensated crust and the buoyant forces that result from the overcompensation cause vertical uplifts. Gravity modelling along some other profiles also suggests similar crustal thickening under Wagad uplift<sup>5</sup>, which in general is also confirmed from special processing of seismic records along Mundra–Adesar profile<sup>16</sup> and receiver function analysis of earthquake records<sup>17</sup>. The gravity highs H3 and H5 in the northern part of Kutch are circular, similar to those observed over volcanic plugs of Deccan trap in Saurashtra<sup>18,19</sup>. They can be caused by the basement uplift or some high-density body at the basement. Modelling of Bouguer anomaly of Pachham island suggests a subsurface high-density body of 2800 kg/m<sup>3</sup> (Figure 6) which represents subsurface volcanic rocks. This body may represent a volcanic plug similar to those exposed in Saurashtra or Deccan trap flows occupying high lands. However, the former appears to be more likely. The volcanic plug-like body suggests that these rocks might have formed as a result of crystallization of primary magma reaching the surface from the upper mantle depth and in quick succession, before volcanism shifted to Saurashtra due to India's rapid northward movement. Incidentally, the location of these isolated volcanic rocks close to the Kutch rift faults cannot rule out their affinity to the rift phase magmatism<sup>20</sup>. However, their association with the Deccan volcanism seems to be reasonable as alkaline magmatic rocks, similar to those reported from volcanic plugs of Deccan trap in Saurashtra<sup>5</sup>, have been reported from different parts of Kutch. These volcanic rocks would then represent the earliest phase of Deccan volcanism from Reunion hot spot activity towards the north of

Kutch mainland. The exposures of Deccan trap in the southern part of Kutch and some recent reports of occurrences of Deccan trap in the northern part near Pachham island by Geological Survey of India, suggest that this may be a possibility.

The Bhuj earthquake of 26 January 2001 and its aftershocks of magnitude greater than four coincide with the intersection of thrust faults F1, F4 and gravity trends H2 oriented NW–SE and NE1 oriented NE–SW (Figure 2). The NW–SE trend appears to represent a strike slip fault along which the Mesozoic sediments of the KMU have shifted northward to occupy Wagad uplift. The field evidences for a strike slip fault at the western boundary of Wagad uplift near Manfara have also been reported<sup>21</sup>. Satellite imagery<sup>22</sup> reflects a large NW–SE lineament in this section extending southwards along the western margin of the Mesozoic sediments in northern Saurashtra (inset, Figure 1). Northwards, it joins with the Khavda fault (Figure 1) and extends further northwards towards the western boundary of the Indian plate. Seismic activities along NW–SE trends north of Kutch have been reported<sup>23</sup>. Though the Bhuj earthquake did not result in any morphological deformation unlike the 1819 Kutch earthquake (Allah bund) and its fault ruptures could not be located, surface manifestations in the form of mud volcanoes/craters and lateral spreads are many<sup>24–26</sup>. It may be noted that the two centres of gravity lows in the isostatic regional map (A and B, Figure 4) are separated by a NW–SE trend, indicating the deep-seated nature of this trend. The NW–SE is a regional trend of the Indian plate, which was developed along the dominant Dharwarian trend with the break-up of Africa from Indian plate during middle Jurassic–late Cretaceous and was reactivated when Indian plate collided with the Eurasian plate during early Tertiary time<sup>1</sup>. These NW–SE trends might have provided excellent conduits for the migrating stress from the active plate boundary. The abnormal stress accumulation by local stress (isostatic overcompensations) and migrated stress from converging plate boundary towards the Kutch, and their further accentuation due to large-scale sediment deposition and subsidence at Indus cone<sup>27</sup> west of it appears to be responsible for the present-day seismicity in Kutch. Similar, positive correlations between seismicity and isostatic anomalies have also been reported from the Iranian plateau<sup>28</sup>.

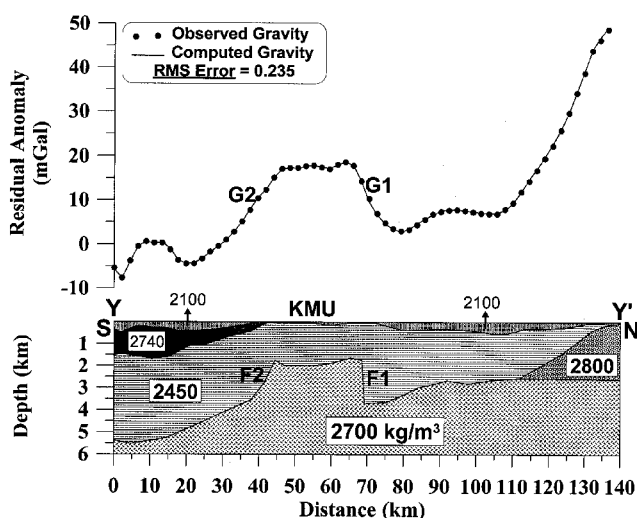


**Figure 6.** Residual Bouguer anomaly and shallow section along profile YY' (Figure 2) and basement uplift of 2–3 km under KMU along margin faults F1 and F2 (Figure 1).

1. Besse, J. and Courtillot, V., *J. Geophys. Res.*, 1988, **93**, 11791–11808.
2. Biswas, S. K., *Tectonophysics*, 1987, **135**, 307–327.
3. Merh, S. S., *J. Geol. Soc. India*, 1995, 1–222.
4. Raval, U., *Curr. Sci.*, 2001, **81**, 809–815.
5. Mishra, D. C., Chandrasekhar, D. V. and Singh, B., International Conference on Seismic Hazard with Particular Reference to Bhuj Earthquake of 26 January 2001, 3–5 October 2001, New Delhi.
6. Oldham, R. D., *Mem. Geol. Surv. India*, 1926, 46, 1–77.
7. Chung, W. Y. and Gao, H., *Tectonophysics*, 1995, **242**, 281–292.

8. Rajendran, C. P. and Rajendran, K., *Bull. Seismol. Soc. Am.*, 2001, **91**, 407–426.
9. Lal, B. B., *Sci. Age*, 1984, **8**, 8–9.
10. *Seismic Zoning Map of India*, Bureau of India Standards, New Delhi, 1986.
11. *Bouguer Anomaly Map of India*, National Geophysical Research Institute, Hyderabad, 1978, pp. 1–15.
12. Subba Rao, D. V., *Geophys. Res. Lett.*, 1996, **23**, 3543–3546.
13. Gupta, H. K. *et al.*, *J. Geol. Soc. India*, 2001, **57**, 275–278.
14. Srinivasan, S. and Khar, B. M., Proceedings of Petrotech-95, Technology Trends in Petroleum Industry, New Delhi, 1995, pp. 1–16.
15. Webring, M., *US Geol. Surv. Open File Rep.*, 1985, **29**, 85–122.
16. Reddy, P. R., Sarkar, D., Sain, K. and Mooney, W. D., Unpublished Report, USGS, Menlo Park, USA, 2001, pp. 35–44.
17. Ravi Kumar, M., Saul, J., Sarkar, D. and Kind, R., *Geophys. Res. Lett.*, 2001, **28**, 1339–1342.
18. Mishra, D. C. *et al.*, *Curr. Sci.*, 2001, **80**, 1059–1067.
19. Chandrasekhar, D. V., Mishra, D. C., Poornachandra Rao, G. V. S. and Mallikharjuna Rao, J., *Earth Planet. Sci. Lett.*, 2002, **201**, 277–291.
20. Mishra, D. C., *IUGG 99*, 1999, A113.
21. Seeber, R., *USGS, web site*, 28 February 2001.
22. IRS-1D, *Satellite Thematic Map of Gujarat*, NRSA, Hyderabad, 1998.
23. Kazmi, A. H., *Geodynamics of Pakistan* (eds Farah, A. and Dejong, K. A.), Geological Survey of Pakistan, 1979, pp. 285–304.
24. Karanth, R. V. *et al.*, *J. Geol. Soc. India*, 2001, **58**, 193–202.
25. Rajendran, K., Rajendran, C. P., Mahesh Thakkar and Tuttle, Martita P., *Curr. Sci.*, 2001, **80**, 1397–1405.
26. Bendick, R. *et al.*, *Seismol. Res. Lett.*, 2001, **72**, 328–335.
27. Clift, P., Shimizu, N. and Layne, G., *EOS Trans. AGU*, 2000, **81**, 277.
28. Zamani, A. and Hashemi, N., *Tectonophysics*, 2000, **327**, 25–36.

ACKNOWLEDGEMENTS. We thank the Director, NGRI, Hyderabad for his permission to publish this work. Thanks are also due to Mr R. S. Rajesh for help in data acquisition. We also thank the two anonymous reviewers and Dr Kusala Rajendran for their constructive suggestions.

Received 5 November 2001; revised accepted 7 June 2002

## Negative $\delta^{13}\text{C}$ excursion and anoxia at the Permo-Triassic boundary in the Tethys Sea

Prosenjit Ghosh<sup>†</sup>, S. K. Bhattacharya<sup>†,\*</sup>,  
A. D. Shukla<sup>†</sup>, P. N. Shukla<sup>†</sup>, N. Bhandari<sup>‡</sup>,  
G. Parthasarathy<sup>#</sup> and A. C. Kunwar<sup>†</sup>

<sup>†</sup>Physical Research Laboratory, Navrangpura, Ahmedabad 380 009, India

<sup>#</sup>National Geophysical Research Institute, Hyderabad 500 007, India

<sup>‡</sup>Indian Institute of Chemical Technology, Hyderabad 500 007, India

**The Permian–Triassic (P–T) sections in Spiti valley, Himalaya represent sedimentary deposits of a shallow sea and show a sharp negative transition of  $\delta^{13}\text{C}$  in total organic matter, kerogen fraction and carbonate phase. This excursion occurs across the upper part of the Permian shale culminating in a ferruginous band, which marks the peak of anoxicity after a period of generally low-oxygenated condition in the basin, as inferred on the basis of trace element analysis. Presence of carbon isotopic shift along with anoxia is similar to that observed in many P–T sections over the globe and suggests that Permo-Triassic transitional records of the Neo-Tethys are preserved in the ferruginous band of the Spiti valley sections.**

THE Permian–Triassic (P–T) transition represents a time of remarkable changes in the Phanerozoic when nearly 90% of shelly marine genera were wiped out<sup>1</sup>. It is characterized by diverse isotopic and chemical markers interpreted variously to indicate catastrophic events such as extra-terrestrial impacts<sup>2–6</sup>, marine regression<sup>7</sup>, climate

change<sup>8,9</sup>, oceanic anoxia<sup>10</sup>, overturning of the sea<sup>11</sup> and volcanism<sup>12</sup>. A sudden excursion of  $\delta^{13}\text{C}$  of kerogen and organic material has been observed in a few sections across the boundary<sup>13,14</sup>. Recently, Musashi *et al.*<sup>15</sup> confirmed this excursion in the sedimentary organic matter and inorganic carbonates collected across P–T boundary sections of south-western Japan, indicating that it may be a global phenomenon representing an important event horizon.

Permian and Triassic sediments in the extra-peninsular India were deposited in the western periphery of Neo-Tethys, a confined body of water separated from Palaeo-Tethys. These sediments are exposed along Guryul ravine (Kashmir), Lahaul valley and Spiti valley of northwest Himalaya. In the Spiti valley, a thin (1–10 cm) ferruginous band separates the Permian shale from the Triassic limestone<sup>2,16</sup>. In spite of significant advances in chemostratigraphy, inter-basinal correlation among the Phanerozoic sequences is difficult to establish due to problems associated with doubtful faunal record, presence of hiatus in sedimentary deposition, variable sampling resolution, absence of facies control, etc. Well-preserved shale–carbonate sequence straddling the Permian and Triassic in Spiti Himalaya, provides an opportunity to establish the geochemical changes across the P–T boundary (PTB) within a broad global chemostratigraphic framework. In addition, since these sediments formed in a sea, the  $\delta^{13}\text{C}$  of organic matter should reflect the variation of surface-water productivity and dissolved  $\text{CO}_2$  concentration across the P–T transition and may serve as global marker.

With this view, we have analysed the carbon isotope ratio of organic matter and marine carbonates across the PTB in shale and limestone sequences from Attargoo, Guling and Lalung sections of the Spiti valley.

\*For correspondence. (e-mail: bhatta@prl.ernet.in)